DOI: 10.1002/chem.200800092

Protonated Macrobicyclic Hosts Containing Pyridine Head Units for Anion Recognition

David Esteban-Gómez,*[a] Carlos Platas-Iglesias,[a] Andrés de Blas,[a] Luigi Fabbrizzi,[b] and Teresa Rodríguez-Blas*[a]

Abstract: In this paper, we report two macrobicyclic receptors containing pyridine head units derived from 1,10-diaza-15-crown[5] (L^1) or 4,13-diaza-18-crown[6] (L^2) that can be protonated in MeCN and used for anion recognition. The interaction of these protonated lateral macrobicycles with different anions has been investigated by means of spectrophotometric titrations in MeCN. The association constants for the complexes of halide anions with the protonated macrobicycles follow the sequences $Cl^- > Br^- > I^- > F^-$ (L^1) and $Cl^- > F^- > I^- > Br^-$ (L^2), whereby an increase of more than two logarithmic units is observed from F^- to Cl^- for the binding constants of the receptor derived from L^1. The association constants also indicate an important degree of selectivity of these macrobicyclic receptors for Cl^- over Br^- or I^-. The X-ray crystal structure analyses of the chloride and bromide complexes confirms the formation of the envisaged supramolecular complexes. Moreover, the binding constants indicate that these receptors present a high sulfate-to-nitrate binding selectivity. The stability trend observed for the recognition of halide anions by the macrobicycles presented herein as well as the sulfate-to-nitrate binding selectivity have been rationalised by means of DFT calculations at the B3LYP/LanL2DZ level. These studies indicate that the especially high binding selectivity for Cl^- is the result of the optimum fit between the protonated macrobicyclic cavity and the size of the anion, whereas the sulfate-to-nitrate selectivity results from shape complementarity between the hydrogen-binding acceptor sites on sulfate and the hydrogen-bond donors of the macrobicycle.

Keywords: anion recognition · anions · hydrogen bonds · macrocycles · supramolecular chemistry

Introduction

Anion recognition continues to receive considerable attention from the supramolecular chemistry community.[1] Progress in this area has lead to the design of a variety of selective receptors with very different purposes, that is, binding and transport of biologically important compounds,[2,3] application in the catalysis of organic reactions,[4] anion-template reactions,[5,6] analytical chemistry[7] and the synthesis of receptors for selective anion transport and extraction.[8]

Amide,[9,10] polyamine[11] or polyammonium[12–14] macrocyclic and macrobicyclic receptors have been employed for anion coordination. It is known that the strength and selectivity of complexation between anions and polyammonium receptors depends both on electrostatic interactions (charge) and structural effects (topology and/or dimensionality),[15,16] so that the modification of size and shape of macrocyclic receptors can be used to control the selectivity sequence through topological complementarity by arranging the binding groups conveniently in a convergent and rigid manner around the anions.[17] Moreover, the geometry of the anion is also an important feature to be considered in receptor design to achieve binding selectivity. No preference for a specific geometry or a coordination number is observed for the spherical halide anions, which can fit tetrahedral, octahedral or other polyhedral coordinating environments offered by the polyammonium host.[17,18] On the other hand, oxoanions, such as NO_3^- (trigonal planar) or HSO_4^- and $H_2PO_4^-$ (tetrahedral), require geometrically defined co-

[a] Dr. D. Esteban-Gómez, Dr. C. Platas-Iglesias, Dr. A. de Blas, Dr. T. Rodríguez-Blas
Dpto. Química Fundamental
Facultade de Ciencias, Universidade da Coruña
Campus da Zapateira s/n, 15071A Coruña (Spain)
Fax: (+34) 981-167065
E-mail: mayter@udc.es

[b] Prof. L. Fabbrizzi
Dipartimento di Chimica Generale
Università di Pavia
via Taramelli 12, 27100 Pavia (Italy)

Supporting information for this article is available on the WWW under http://www.chemeurj.org/ or from the author.

ordination environments, and selectivity can be achieved by taking account of their geometrical features.[19,20]

Herein, we report an investigation of the anion-binding affinity of the lateral macrobicycles L^1 and L^2 (Scheme 1) as

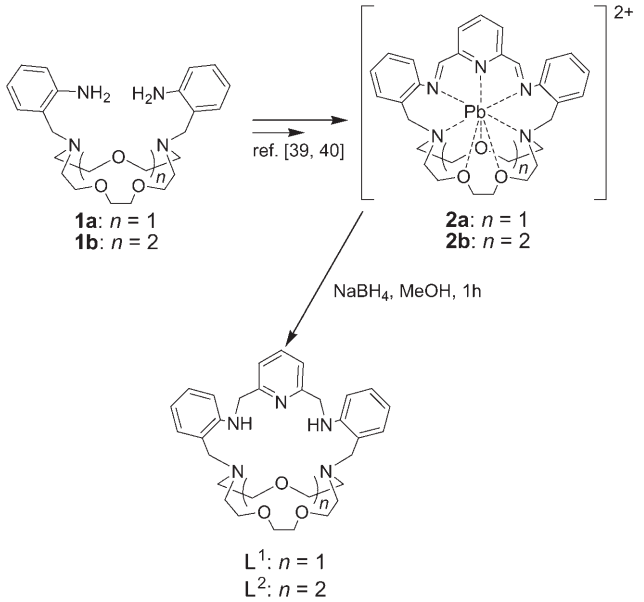

Scheme 1. Syntheses of receptors L^1 and L^2.

their protonated forms. Lateral macrobicycles are dissymmetrical molecules structurally based on the combination of two different binding subunits, a chelating one and a macrocyclic one.[21] Considering the peculiar structural features shown by lateral macrobicycles, one could anticipate that such macropolycyclic architectures offer a range of interesting and potentially useful molecular recognition properties for both cations and anions owing to the presence of convergent binding groups that are specially arranged to match the functionality of the guest molecule. Moreover, they offer the advantage of being preorganised and therefore capable of profiting from the thermodynamic macrobicyclic effect. It has been shown that lateral macrobicycles behave as very versatile receptors that can be used as platforms to obtain homo- and heterometallic dinuclear complexes with many different aims, that is, to induce processes of "push–pull" dimetallic substrate activation[22] and as receptors for organic molecules[23] or contact ion pairs.[24,25] However, to date the recognition of anions by this type of receptor has remained much less explored than cation recognition.[26] Receptors L^1 and L^2 (Scheme 1) contain a pyridine head unit and two tertiary amine nitrogen atoms that may be all protonated and thus used for anion recognition.[18,27] Furthermore, the two secondary amine groups may act as additional hydrogen-bond donors, as previously observed for different polyaza macrocyclic receptors.[28] These NH groups can be hardly protonated owing to delocalisation of the amine lone pair into the aryl ring. Indeed, electrostatic interactions between a negatively charged anion and a positively charged ligand can influence and enhance binding.[12] Protonation of macrobicycles L^1 and L^2 is expected to provide up to five hydrogen-bond donors arranged in a somewhat spherical fashion. Moreover, the presence of the protonated amine moieties is expected to play a key role in anion complexation, providing both hydrogen donor subunits and positively charged binding sites.

The combination of a pyridine ring with amide groups is frequently used in anion recognition as a rigid framework in which amide protons are involved in an intramolecular hydrogen bond with the nitrogen atom of the pyridine.[9] This interaction preorganises and polarises the hydrogen-bond donor groups to give a planar subunit with a positive partial charge that shows high affinity for different anions. However, in our case, and to achieve a greater receptor–anion affinity, we have used a more flexible and positively charged moiety by introducing a protonated pyridine and secondary amine groups, instead of amide groups. On the other hand, the crown moiety has been incorporated into our receptors because of its ability to increase their solubility in polar solvents.

Results and Discussion

Synthesis and characterisation of the macrobicyclic receptors: Receptors L^1 and L^2 were easily prepared by reduction of the corresponding Pb^{II} perchlorate complexes of the Schiff-base macrobicyclic precursors (**2a** and **2b**, Scheme 1) with sodium borohydride. The IR spectra of L^1 and L^2 do not show imine stretches, but contain bands attributed to the N–H stretching and bending modes at $\nu = \approx 3250$ and 1605 cm^{-1}, respectively, in agreement with the formation of the expected amine macrobicycles. Moreover, the IR spectra do not show bands corresponding to the ν_{as}(Cl–O) stretching mode of the perchlorate group,[29] indicating that reductive demetallation of **2a** and **2b** has occurred. The FAB mass spectra and ^1H and ^{13}C NMR spectroscopy data, together with elemental analyses (see the Experimental Section) also indicated the formation of the desired macrobicyclic receptors.

Protonation studies: Protonation of L^1 and L^2 has been followed by NMR and UV-visible spectroscopies in acetonitrile at room temperature. Figure 1 shows a family of UV-visible spectra recorded during the course of a titration of a 10^{-4} M solution of the corresponding macrobicyclic receptor with trifluoroacetic acid in CH_3CN. The UV-visible spectrum of the free receptor L^1 (Figure 1) shows two absorption bands with maxima at $\lambda = 252$ nm ($\varepsilon = (24000 \pm 400)$ $dm^3 mol^{-1} cm^{-1}$) and 291 nm ($\varepsilon = (8500 \pm 400)$ $dm^3 mol^{-1} cm^{-1}$), which correspond to E_2 and $B\pi^* \leftarrow \pi$ bands of the aromatic rings, respectively.[30] The spectrum of L^2 (Figure 1) is similar to that of L^1, and displays bands at $\lambda = 251$ nm ($\varepsilon = (24600 \pm 300)$ $dm^3 mol^{-1} cm^{-1}$) and 296 nm ($\varepsilon = (70200 \pm 300)$ $dm^3 mol^{-1} cm^{-1}$), together with a shoulder at 267 nm. Upon addition of trifluoroacetic acid to solutions

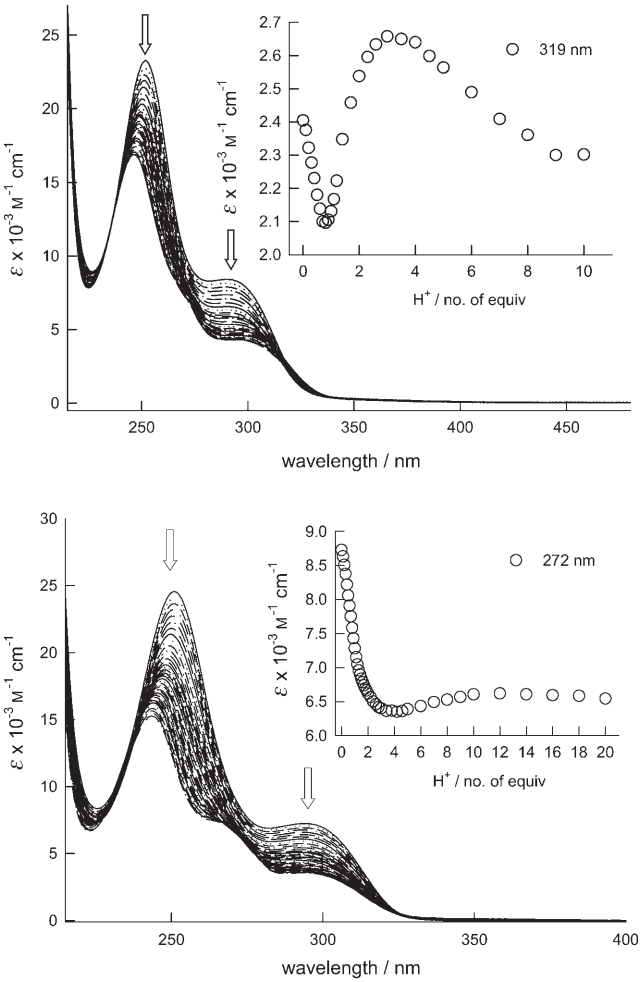

Figure 1. UV-visible absorption spectra recorded over the course of the titration of a 10^{-4} M solution of L^1 (top) or L^2 (bottom) with a standard solution of CF_3COOH in acetonitrile. Insets: titration profiles at selected wavelengths.

of the macrobicycles in acetonitrile, the intensity of both absorption maxima decreases while the band at higher energy shifts to shorter wavelengths. The titration profiles (Figure 1) clearly show two inflection points at CF_3COOH/L molar ratios of 1:1 and 2:1, which indicates the occurrence of two protonation steps. Addition of excess trifluoroacetic acid causes further changes in the titration profile, which suggests a third protonation process. The data can be interpreted on the basis of Equations (1) to (3):

$$L+H^+ \rightleftharpoons [HL]^+ \qquad \beta_{11} \tag{1}$$

$$L+2\,H^+ \rightleftharpoons [H_2L]^{2+} \qquad \beta_{12} \tag{2}$$

$$L+3\,H^+ \rightleftharpoons [H_3L]^{3+} \qquad \beta_{13} \tag{3}$$

A non-linear least-squares treatment of the titration profiles provides the following $\log\beta$ values: $\log\beta_{11}=5.85(4)$, $\log\beta_{12}=9.7(1)$ and $\log\beta_{13}=12.76(9)$ (L^1) and $\log\beta_{11}=6.9(1)$, $\log\beta_{12}=11.0(1)$ and $\log\beta_{13}=14.2(1)$ (L^2). The $\log\beta_{11}$ values indicate that the first protonation step is more favourable in the case of L^2, which suggests that the larger macrocyclic cavity size of L^2, compared with that of L^1, allows a stronger intramolecular hydrogen-bonding interaction in the $[HL^2]^+$ species.

Protonation of the receptors was also monitored by ^{1}H NMR spectroscopy. Addition of two equivalents of CF_3COOH to a 5×10^{-3} M solution of L^1 in CD_3CN causes drastic changes in the ^{1}H NMR spectrum. The signal attributed to the benzylic protons, which is observed at $\delta=3.58$ ppm in the spectrum of L^1, experiences an important downfield shift to $\delta=4.25$ ppm upon addition of two equivalents of acid (Figure 2a and b). The signals attributed to the

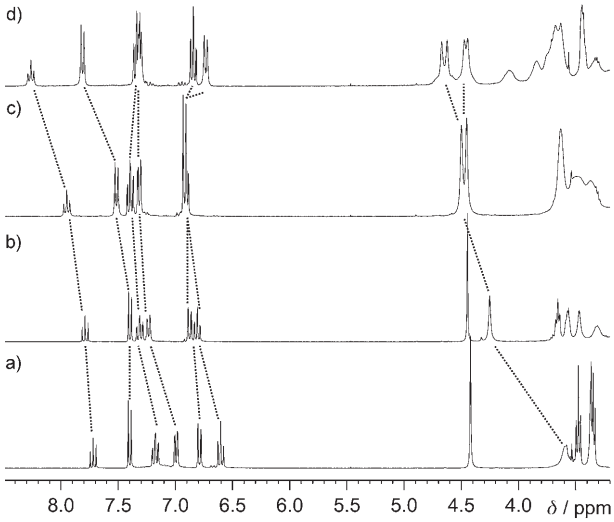

Figure 2. ^{1}H NMR spectra (300 MHz, 298 K, CD_3CN) of a) a 5×10^{-3} M solution of L^1, b) the same solution after the addition of 2 equiv CF_3COOH, c) after the addition of 8 equiv CF_3COOH and d) after the addition of 8 equiv CF_3COOH and 1 equiv nBu$_4$N$^+$Cl$^-$.

protons of the phenyl units also shift downfield by 0.08–0.24 ppm upon addition of two equivalents of acid, whereas the proton signals of the pyridine units are less affected. These results suggest that the first two protonation steps correspond to the protonation of the two amine nitrogen atoms of the crown moiety. A similar situation has been observed for different Schiff-base lateral macrobicycles derived from crown ethers.[31] Addition of excess CF_3COOH (8 equiv) causes further changes in the ^{1}H NMR spectrum (Figure 2). In particular, the proton signals of the pyridine units undergo a downfield shift of 0.12–0.16 ppm, which suggests that the third process involves the protonation of the pyridine nitrogen atom. According to the protonation constants determined from UV-visible titrations, under these conditions the major species in solution is the triprotonated form of the ligand (>97%).

Anion-binding studies: The interaction of the protonated receptors with different anions has been followed by means of spectrophotometric titrations on 10^{-4} M solutions of the re-

ceptors in acetonitrile in the presence of CF_3COOH (15 equiv). Under these conditions, the major species in solution is the triprotonated form of the corresponding macrobicycle (≈60% for L^1 and ≈70% for L^2). Owing to the low value of the third protonation constant, a very large excess of acid is required to ensure triprotonation of the receptors at a concentration of 10^{-4} M. For instance, L^1 requires ≈200 equivalents of acid to attain a concentration of $[H_3L^1]^{3+}$ of ≈95%. Thus, the obtained binding constants are weighted values of the binding constants with the different species present in solution, as shown in Equations (4) and (5):

$$[H_nL]^{n+}+X^- \rightleftharpoons [H_nLX]^{(n-1)+} \qquad K_{11} \tag{4}$$

$$[H_nL]^{n+}+A^- \rightleftharpoons [H_nLA]^{(n-1)+} \qquad K_{11} \tag{5}$$

in which X and A represent a halide anion or an oxoanion, respectively. Addition of halide anions as their tetrabutylammonium salts causes appreciable modifications of the spectral pattern. The tetrabutylammonium cation is highly diffuse and does not bind to crown ethers.[32] Thus, the binding constants observed with the tetrabutylammonium salts reflect the receptor–anion affinity. The family of UV-visible spectra recorded over the course of the titrations of L^1 and L^2 with Cl^- are shown in Figure 3. Addition of Cl^- increases the intensity of the absorption maxima at ≈245 and 293 nm, and in the case of L^2, the intensity of the shoulder at 267 nm increases as well. The titration profiles (Figure 3) indicate a 1:1 stoichiometry for the receptor–Cl^- interaction. Addition of F^-, Br^- or I^- induces similar spectral changes (Figure 4). A similar situation occurs for different oxoanions, such as ClO_4^-, NO_3^-, HPO_4^{2-} and HSO_4^- (Figure 4). All of the titration data gave best-fit host-to-guest stoichiometries of 1:1, in agreement with Job plots (see the Supporting Information) indicating a maximum $\Delta\varepsilon$ at $0.5=[L]/([L]+[A^-])$. In contrast, no spectral changes were observed when the neutral hosts were titrated with the anions investigated in this work. Thus, the neutral forms of macrobicycles L^1 and L^2 appear to have a negligible affinity for these anions.

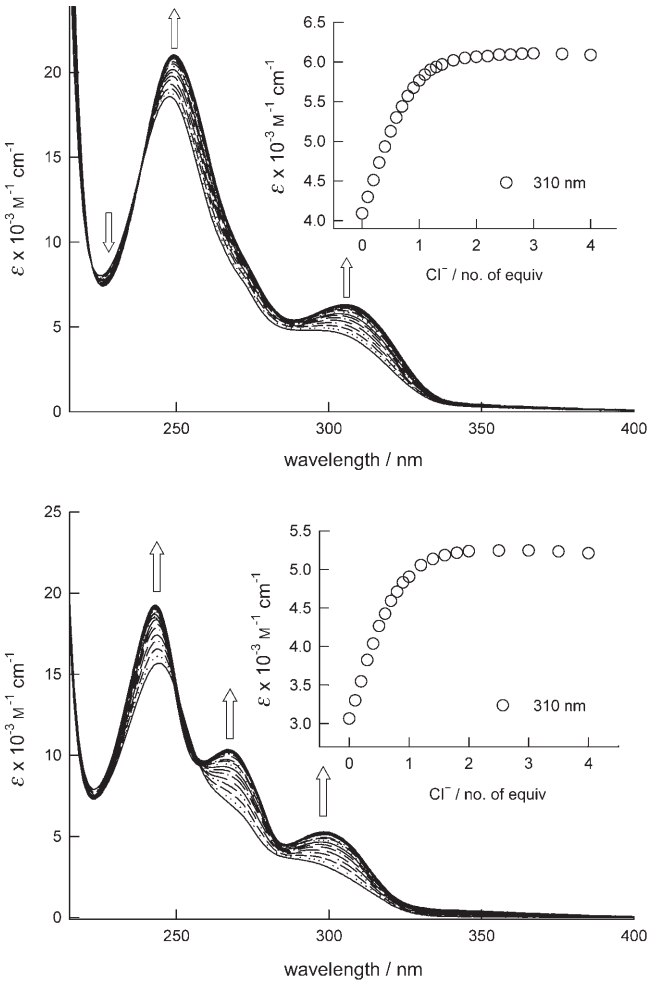

Figure 3. UV-visible absorption spectra recorded over the course of the titration of a 10^{-4} M solution of L^1 (top) or L^2 (bottom) in acetonitrile with a standard solution of $nBu_4N^+Cl^-$ in the presence of 15 equiv CF_3COOH. Insets: titration profiles at selected wavelengths.

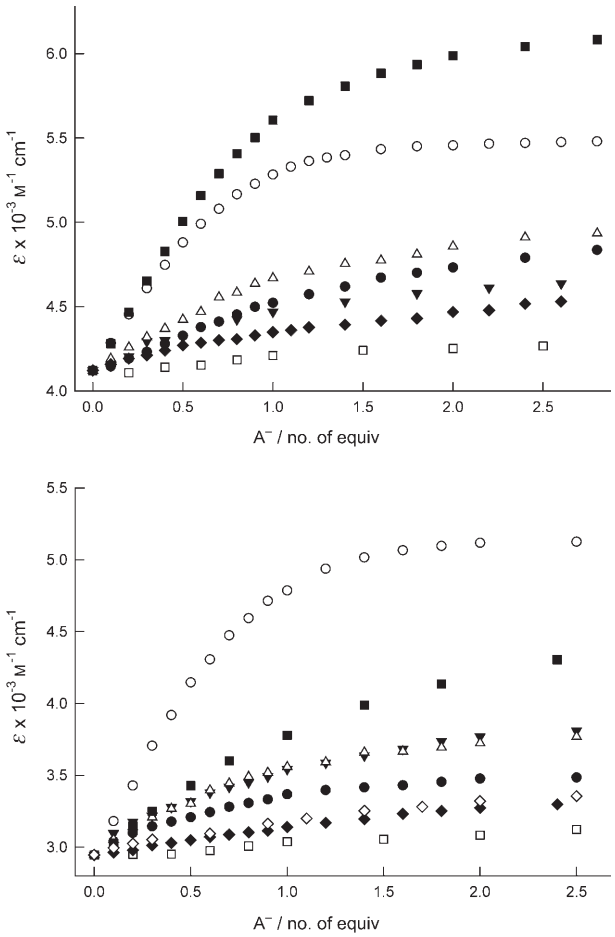

Figure 4. UV-visible absorption spectral changes at 300 nm observed during the course of the titration of F^- (●), Cl^- (○), Br^- (▼), I^- (△), HSO_4^- (■), ClO_4^- (□) and $H_2PO_4^-$ (◆) with standard 10^{-4} M solutions of L^1 (top) and L^2 (bottom) in acetonitrile in the presence of 15 equiv CF_3COOH.

^{1}H NMR spectroscopy confirms the recognition of halide anions by these macrobicyclic receptors. Indeed, the addition of one equivalent of Cl^- to a solution of $[H_3L^1]^{3+}$ (Figure 2c and d) induces significant changes in the position of the signals attributed to the pyridine protons, which shift downfield by ≈ 0.30 ppm. The signals attributed to the aromatic protons of the phenyl groups experience significant highfield shifts. The spectral region between $\delta = 2.5$ and 4.7 ppm becomes more complicated upon addition of Cl^-, probably because complexation of the anion increases the rigidity of the receptor. Lowering the temperature to 273 K results in a more clearly resolved spectrum that is in agreement with an effective C_s symmetry in solution (see the Supporting Information). Moreover, no substantial changes in the spectrum have been observed upon cooling at 233 K, which suggests symmetric binding of the guest to the macrobicycle.

Non-linear least-squares fits of the UV-visible titration profiles allowed us to determine the binding constants listed in Tables 1 and 2. Among the different anions investigated, the highest affinity of receptors L^1 and L^2 is observed with chloride. The association constants for the interaction of halide anions with the protonated forms of macrobicycles L^1 and L^2 vary in the following order (Table 1) $Cl^- > Br^- > I^- > F^-$ (L^1) and $Cl^- > F^- > I^- > Br^-$ (L^2), with an increase in the binding constants by more than two logarithmic units from F^- to Cl^- in the case of L^1. This implies that the cavity size of both receptors is suitable for complexation with Cl^-. An especially high affinity for Cl^- versus F^- has been previously observed for quaternised-amine macrocycles.[15,33] However, the binding trend observed for L^1 and L^2 towards halide anions differs from that observed for polyamide cryptands containing pyridine head units, which display the highest affinity for F^-.[9e] The association constants given in Table 1 also indicate an important degree of selectivity of these macrobicyclic receptors for Cl^- over Br^- or I^-. A comparison of the solid-state structures of $[(H_3L^1)Cl]^{2+}$ and $[(H_3L^1)Br]^{2+}$ and the DFT calculations described below suggests that this can be, at least in part, attributed to a best match between the anion guest and the macrobicyclic cavity for Cl^-. The lower stability of the F^- complexes compared with those of Cl^- can be ascribed to the small size of the anion, which does not allow interaction with the five hydrogen-bonding donor sites of the protonated macrobicycle (see the DFT calculations below).

Table 1. Binding constants ($\log K$ values) of the halide adducts with the protonated forms of macrobicycles L^1 and L^2 obtained from spectrophotometric titrations in CH_3CN at 25 °C. $\log K$ refers to $[H_nL]^{n+} + X^- \rightleftarrows [H_nLX]^{(n-1)+}$.[a]

	F^-	Cl^-	Br^-	I^-
L^1	3.11(3)	5.15(1)	4.09(1)	3.82(2)
L^2	4.22(3)	5.40(5)	3.75(1)	4.09(2)

[a] The errors given correspond to one statistical deviation.

Table 2. Binding constants ($\log K$ values) of the oxoanion adducts with the protonated forms of macrobicycles L^1 and L^2 obtained from spectrophotometric titrations in CH_3CN at 25 °C. $\log K$ refers to $[H_nL]^{n+} + A^- \rightleftarrows [H_nLA]^{(n-1)+}$.[a]

	HSO_4^-	$H_2PO_4^-$	ClO_4^-	NO_3^-
L^1	4.72(1)	3.78(5)	3.13(4)	< 1
L^2	4.02(1)	3.48(3)	3.23(2)	3.36(1)

[a] The errors given correspond to one statistical deviation.

The binding constants reported in Table 2 indicate that the affinity of these macrobicycles to NO_3^- critically depends on the size of the crown moiety. Indeed, receptor L^1 shows very weak binding to this anion, whereas L^2 shows a rather strong interaction with NO_3^-. This is probably because a larger size of the crown moiety fragment results in a longer distance between the protonated pivotal nitrogen atoms, so that the NO_3^- anion can fit comfortably inside the macrobicyclic cavity. The values shown in Table 2 also indicate that these receptors exhibit a significant selectivity for sulfate over the other oxoanions studied. The selectivity of sulfate over phosphate, perchlorate and nitrate is particularly important in the case of L^1. ^{1}H NMR spectroscopy confirms the binding of $[H_3L^1]^{3+}$ to HSO_4^-. The addition of HSO_4^- (1 equiv) to a solution of $[H_3L^1]^{3+}$ (Figure 5) significantly changes the position of the signals attributed to the pyridine protons, which shift downfield by 0.36 ppm. The signals attributed to the aromatic protons of the phenyl groups also experience significant shifts. The ^{1}H NMR spectra of the adducts formed by $[H_3L^1]^{3+}$ with Cl^- (Figure 2d) and HSO_4^- (Figure 5) are substantially different, which indicates that the ^{1}H signals of the proton nuclei of the macrobicycle are sensitive to the shape of the bound anion. The selectivity of L^1 for sulfate over nitrate could arise from the shape complementarity between the hydrogen-binding sites

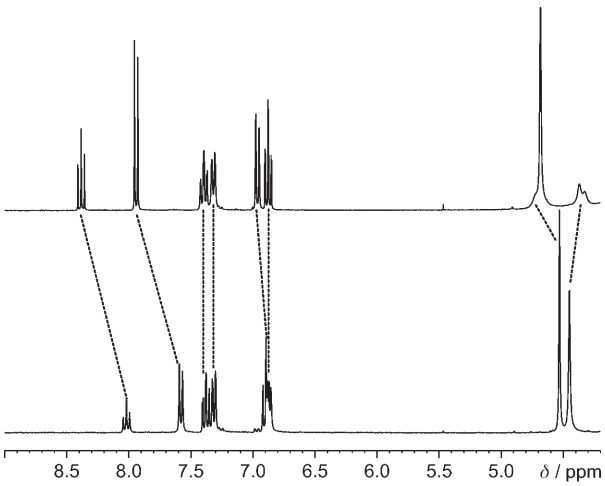

Figure 5. ^{1}H NMR spectra (300 MHz, 298 K, CD_3CN) of a 2×10^{-3} M solution of L^1 after the addition of 8 equiv CF_3COOH (bottom) and the same solution after the addition of 1 equiv nBu$_4$N$^+$HSO$_4^-$ (top).

on HSO_4^- and the hydrogen-bond donors of the macrobicycle.

X-ray crystal structure analyses of the chloride and bromide complexes of the polyammonium receptor $[H_3L^1]^{3+}$ confirm the formation of genuine 1:1 supramolecular complexes. Single crystals of formula $[(H_3L^1)Cl]Cl\cdot(ClO_4)$ (**1**) and $[(H_3L^1)Br](Br)_2\cdot MeOH$ (**2**) suitable for X-ray diffraction were grown by slow evaporation of a solution of L^1 in MeOH in the presence of excess aqueous HCl or HBr. In the case of the chloride adduct, perchloric acid was also added to favour crystallisation. As shown in Figure 6, the organic receptor crystallises in its triprotonated form, and one halide anion is included in its cavity. This endocyclic halide anion is held within the macrobicyclic cavity by four NH···X hydrogen bonds involving the anion and the two *endo*-oriented protonated pivotal nitrogen atoms, the protonated pyridine nitrogen atom and one of the secondary aniline groups. Selected geometrical parameters for NH···X (X = Cl^- or Br^-) interactions are given in Table 3. The fifth NH group of the macrobicyclic cage N3 points outward and is involved in a weak hydrogen-bonding interaction with an exocyclic halide anion (**1**: N3···Cl2 3.411(2) Å, N3–H(3N) 0.82(3) Å, H(3N)···Cl2 2.73(3) Å, N3–H(3N)···Cl2 142(3)°; **2**: N3···Br2 3.460(4) Å, N3–H(3N) 0.87(6) Å, H(3N)···Br2 2.75(6) Å, N3–H(3N)···Br2 140(5)°). The counterions and solvent molecules are associated with each other through hydrogen-bonding networks that stabilise the crystal packing.

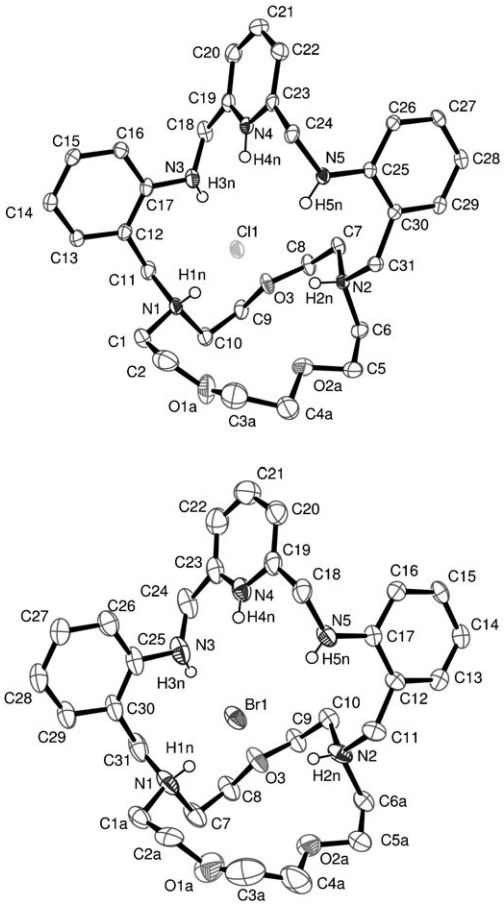

Figure 6. X-ray crystal structure of $[(H_3L^1)Cl]^{2+}$ in **1** (top) and $[(H_3L^1)Br]^{2+}$ in **2** (bottom). Most of the hydrogen atoms and disorder have been omitted for clarity. The ORTEP plot is at the 50% probability level.

Table 3. Selected hydrogen-bonding data [Å and °] of the X-ray structures of the adducts $[(H_3L^1)Cl]^{2+}$ and $[(H_3L^1)Br]^{2+}$.[a]

X	Cl	Br
N1···X	3.221(3)	3.379(4)
X···H1	2.39(3)	2.55(6)
N1–H1···X	169(3)	162(5)
N2···X	3.283(2)	3.457(4)
X···H2	2.52(3)	2.76(6)
N2–H2···X	155(3)	145(5)
N4···X	3.468(2)	3.691(5)
X···H4	2.65(3)	2.91(6)
N4–H4···X	161(3)	171(6)
N5···X	3.118(2)	3.236(4)
X···H5	2.30(3)	2.57(6)
N5–H5···X	158(3)	162(6)
N1···N2	4.795(3)	4.835(6)
N3···N5	4.961(3)	4.841(6)
X···centroid[b]	1.576	1.845

[a] See Figure 6 for the numbering scheme. [b] The position of the centroid is defined by the five nitrogen atoms of the macrobicyclic cavity.

The related macrobicyclic ditopic amide ligands reported by Smith et al.[24,25] contain an alkali cation coordinated to the crown moiety, and the halide anion is only involved in a hydrogen-bonding interaction to two amide NH groups. In such cases, the driving force for anion recognition is the formation of a contact ion pair between the anion and the alkali cation. In our polyammonium receptors $[H_3L^1]^{3+}$ and $[H_3L^2]^{3+}$, the electrostatic interaction between the anion and the protonated sites of the macrobicycle appears to be responsible for anion binding.

The aromatic rings of the receptor show a stair-like conformation in both cases. In **1**, the dihedral angle between the pyridine ring and the plane containing the benzyl ring attached to N5 is 84.4(1)°, whereas the angle formed with the plane containing the second aromatic ring is 86.9(1)°. The corresponding values in the bromide adduct (**2**) are 78.4(2) and 75.2(1)°, respectively. These values reflect a somewhat different folding of the receptor owing to the different position of the corresponding halide anion with respect to the centroid of the receptor cavity (Table 3). Moreover, the receptor modifies, to a certain extent, the size of the cavity to maximise interactions between the NH groups of the receptor and the different anion guest. This is confirmed by a comparison of the distances between the three charged nitrogen atoms, which gives an idea of the size of the macrobicyclic cavity: in $[(H_3L^1)Cl]^{2+}$ the N1–N2, N2–N4 and N1–N4 distances are 4.795(6), 5.059(2) and 5.570(3) Å, whereas in $[(H_3L^1)Br]^{2+}$ these distances are 4.835(6), 5.231(6) and 5.732(6) Å, respectively.

DFT calculations: DFT calculations are a powerful tool for the investigation of different supramolecular entities, which includes receptor–anion complexes.[34] Moreover, solid-state structures might be conditioned by crystal-packing forces and intermolecular hydrogen-bonding interactions, and can differ significantly from structures in a liquid solution. With the aim of rationalising the observed stability trends, the different $[(H_3L^1)X^-]^{2+}$ systems (X = F, Cl, Br or I) were characterised by means of DFT calculations performed in vacuo (B3LYP/LanL2DZ model). The calculated geometries for the $[(H_3L^1)Cl]^{2+}$ and $[(H_3L^1)Br]^{2+}$ systems resemble the solid-state structures. However, while in the solid state the anion is held within the macrobicyclic cavity by four NH···X hydrogen bonds, with one of the secondary amine functions involved in a hydrogen-bonding interaction with an exocyclic halide anion, the calculated structures show that the halide anion interacts with the macrobicycle through five NH···X hydrogen bonds involving the two protonated pivotal nitrogen atoms, the protonated pyridine nitrogen atom and the two secondary amine groups (Table 4). However, the situation in solution might be different to that observed in the solid state because the ^{1}H NMR spectra of the Cl^- adduct did not provide any evidence for asymmetric binding of the anion to the macrobicyclic host. A similar situation is also observed in the case of the iodide adduct. The N···X and X···H distances calculated for the Cl^-, Br^- and I^- complexes (Table 4) are in very good agreement with experimental mean distances observed in the solid state for medium-to-strong hydrogen-bonding interactions.[35,36] Hydrogen-bond lengths increase approximately with the ionic radius of the anion, as previously observed for halide complexes with axial macrobicyclic receptors.[17]

Table 4. Hydrogen-bonding data [Å and °] obtained from DFT calculations (B3LYP/LanL2DZ) for the $[(H_3L^1)X^-]^{2+}$ systems (X = F, Cl, Br and I).[a]

X	F	Cl	Br	I
N1···X	2.635	3.219	3.410	3.642
X···H1	1.566	2.172	2.368	2.608
N1–H1···X	173.87	175.02	170.48	167.96
N2···X	3.850	3.317	3.618	3.849
X···H2	3.005	2.377	2.846	3.091
N2–H2···X	139.02	148.84	131.06	130.28
N3···X	2.862	3.253	3.535	3.787
X···H3	2.054	2.438	3.040	3.438
N3–H3···X	134.93	136.93	111.20	102.38
N4···X	2.810	3.131	3.290	3.490
X···H4	1.938	2.303	2.389	2.570
N4–H4···X	141.62	138.03	147.25	150.10
N5···X	2.591	3.201	3.536	3.847
X···H5	1.519	2.171	2.511	2.841
N5–H5···X	173.15	167.66	166.91	162.58
X···Centroid[b]	0.488	1.069	1.721	2.164

[a] See Figure 6 for the numbering scheme. [b] The position of the centroid is defined by the five nitrogen atoms of the macrobicyclic cavity.

The smaller F^- anion is only involved in hydrogen-bonding interactions with four of the five sites of the protonated macrobicycle. Indeed, the calculated N2···F distance (3.85 Å) is considerably longer than the remaining N···F distances, which range from 2.59 to 2.86 Å (Table 4). The latter values are again in good agreement with typical experimental values observed in the solid state.[36] These results agree with the lower stability of the complex formed with F^- compared with that formed with chloride, which is the result of the "misfit" of the very small F^- ion in the cavity. A similar situation has been previously observed for inclusion complexes of F^- into macrobicyclic polyammonium receptors.[37] On the contrary, the higher affinity of a polyamide cryptand containing pyridine head units for F^- over Cl^- appears to be related to a best fit of F^- within the macrobicyclic cavity.[9e]

Halides are spherically shaped anions with a single negative charge. As a result, no preference for a specific geometry or a coordination number is observed for the complexed halides.[38] For these reasons, the different anion sizes and propensity to form hydrogen bonds are the principal characteristics that enables selective recognition of these anions with metal-free receptors. Space-filling models of the calculated structures for the different $[(H_3L^1)X]^{2+}$ systems (X = Cl, Br or I) clearly confirm that the protonated macrobicycle $[H_3L^1]^{3+}$ is especially suited to coordination of Cl^- as a consequence of the nice fit between the macrocyclic cavity and the size of this anion, whereas Br^- and I^- are clearly too large to fit within the macrobicyclic cavity (Figure 7).

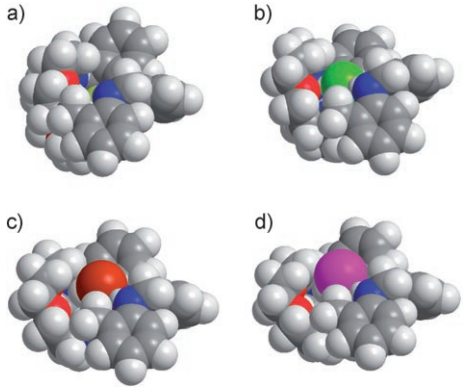

Figure 7. Space-filling representation of the $[(H_3L^1)X]^{2+}$ systems as optimised in vacuo at the B3LYP/LanL2DZ level for X = F (a), Cl (b), Br (c) and I (d).

This is confirmed by the distances between the centroid of the macrobicyclic cavity and the halide anion, which vary in the following order $Cl^- < Br^- < I^-$. These results are again in agreement with the binding trend observed experimentally ($Cl^- > Br^- > I^-$).

To rationalise the sulfate-to-nitrate binding selectivity observed for L^1, the $[(H_3L^1)A]^{2+}$ systems ($A = HSO_4^-$ or NO_3^-) were also characterised by means of DFT calculations (B3LYP/LanL2DZ model). The optimised geometries for both supramolecular complexes are shown in Figure 8. In these systems, the macrobicyclic host adopts a conformation similar to that observed for the corresponding halide complexes. According to our calculations, the HSO_4^- and

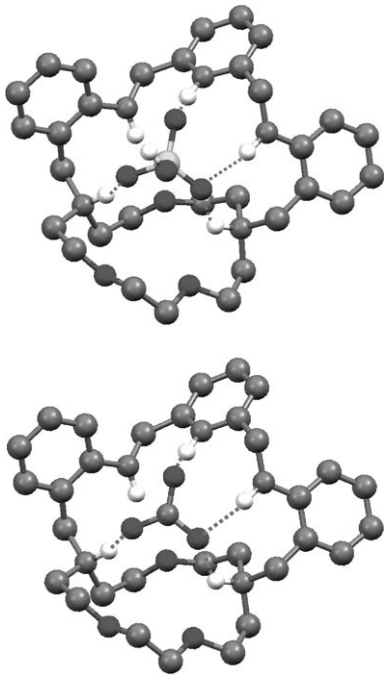

Figure 8. Structures of the $[(H_3L^1)(HSO_4)]^{2+}$ (top) and $[(H_3L^1)(NO_3)]^{2+}$ (bottom) systems obtained from DFT calculations at the B3LYP/LanL2DZ level.

NO_3^- anions are held within the macrobicyclic cavity by four N–H···O hydrogen bonds involving three oxygen atoms of the anion and the three protonated sites of the macrobicycle and one of the secondary amine groups. The calculated structure for the $[(H_3L^1)(HSO_4)]^{2+}$ system shows H···O-S angles that are relatively close to the ideal value of 120°: 105.3, 126.4, 139.8 and 140.5°, in agreement with the strong binding observed in acetonitrile. It is well known that trigonal planar oxyanions, such as NO_3^-, present a clear preference for a coplanar arrangement of the donor sites of the receptor, whereas for tetrahedral oxyanions, such as HSO_4^-, a weak preference is observed for particular H···O-S-O angles.[19,20] The H···O-N-O angles calculated for $[H_3L^1]^{3+}\cdot NO_3^-$ are 57.0, 83.2, 108.0 and 168.0°. These values significantly deviate from the ideal values of 0 and 180°, which is in agreement with a weak interaction between nitrate and the protonated macrobicyclic host.

Conclusion

This work has shown that macrobicyclic receptors containing a mixture of ammonium, pyridinium and secondary aniline hydrogen-bonding donor sites display interesting binding properties towards anions in solution and in the solid state. The relatively high stability of the corresponding complexes results from the presence of a definite spherical cavity, the rigidity of which ensures size selectivity in favour of spherical halide ions. On the other hand, oxoanions are selectively recognised on the basis of their geometrical shape and their capability to accept hydrogen bonds from the tridimensional array of N–H donors of the receptor. Further macrobicyclic receptors of varying geometrical features and designed selectivity can be obtained by following the same convenient synthetic approach.

Experimental Section

Solvents and starting materials: Compounds **2a**·EtOH and **2b** (Scheme 1) were prepared as previously described.[39,40] All other chemicals were purchased from commercial sources and used without further purification. Solvents were of reagent grade purified by the usual methods.

CAUTION! Although we have experienced no difficulties with the perchlorate salts, these should be regarded as potentially explosive and handled with care.[41]

Physical methods: Elemental analyses were carried out on a Carlo Erba 1180 elemental analyzer and FAB-MS were recorded on a FISONS QUATRO mass spectrometer with a Cs ion-gun with a 3-nitrobenzyl alcohol matrix. IR spectra were recorded as KBr discs with a Bruker Vector 22 spectrophotometer. ^{1}H and ^{13}C NMR spectra were recorded on Bruker Avance 300 or 500 spectrometers. NMR spectroscopy assignments were based in part on two-dimensional COSY, HMQC and HMBC experiments. Electronic spectra in the UV/Vis range were recorded at 25 °C on a Perkin–Elmer Lambda 900 UV/Vis spectrophotometer in 1.0 cm quartz cells. The protonation of L^1 and L^2 was studied by means of spectrophotometric titrations of 10^{-4} M solutions of the ligands (10 mL). Typically, aliquots of a fresh standard solution of CF_3COOH (10^{-2} M) in acetonitrile (polarographic grade) were added and the UV/Vis spectra of the samples were recorded. Anion-binding studies were performed on 10^{-4} M solutions of the ligands in acetonitrile in the presence of CF_3COOH (15 equiv, 10 mL). Aliquots of a fresh standard solution (10^{-2} M) of the envisaged anion (as the tetrabutylammonium salt) in the same solvent were added and the UV/Vis spectra of the samples were recorded. All spectrophotometric titration curves were fitted with the HYPERQUAD program.[42] Binding constants were obtained from a simultaneous fit of the UV/Vis absorption spectral changes at 6–8 selected wavelengths in the range 250–325 nm. A minimum of 24 absorbance data points at each of these wavelengths was used.

Receptor L^1: Sodium tetrahydroborate (0.035 g, 0.9 mmol) was added slowly to a stirred solution of **2a**·EtOH (0.206 g, 0.210 mmol) in methanol (100 mL) (Scheme 1). After the addition was complete, the solution was then refluxed for 15 min and then cooled to room temperature. The solvent was removed under reduced pressure to leave a solid residue that was extracted with chloroform (3×30 mL). The solution was concentrated to dryness giving an oily residue that was dissolved in hot acetonitrile (10 mL). After cooling to room temperature, L^1 was obtained as a pale yellow precipitate that was filtered and dried under vacuum over $CaCl_2$ (0.079 g, 71%). M.p. 146–148 °C; ^{1}H NMR (CD_3CN): δ = 7.72 (t, ^3J = 7.7 Hz, 1H; py), 7.40 (d, ^3J = 7.7 Hz, 2H; py), 7.21–7.15 (m, 2H; Ar), 6.99 (dd, ^3J = 7.2 Hz, ^4J = 1.3 Hz, 2H; Ar), 6.79 (d, ^3J = 7.9 Hz, 2H; Ar), 6.65–6.60 (m, 2H; Ar), 4.42 (s, 4H; CH_2), 3.60 (br s 4H; CH_2), 3.48 (t, ^3J = 5.9 Hz, 4H; CH_2), 3.37 (s, 4H; CH_2), 3.35 (t, ^3J = 5.1 Hz, 4H; CH_2), 2.65 (br s, 2H; NH), 2.58–2.54 ppm (m, 8H; CH_2); ^{13}C NMR (CD_3CN): δ = 50.1, 55.6, 56.2, 61.7, 70.0, 70.9, 71.0, 110.7, 116.8, 122.4, 123.8, 129.4, 131.1, 138.1, 149.5, 160.2 ppm; IR (KBr): $\tilde{\nu}$ = 3263 (NH), 1604 (NH), 1592 cm^{-1} (C=N)$_{py}$; FAB-MS: (m/z): 532 $[L^1+H]^+$; elemental analysis calcd (%) for $C_{31}H_{41}N_5O_3$: C 70.0, H 7.7, N 13.1; found: C 69.7, H 7.6, N 12.6.

Receptor L^2: The receptor was prepared as described for L^1 from **2b** (0.210 g, 0.215 mmol) and sodium tetrahydroborate (0.035 g, 0.925 mmol; Scheme 1). Yield: 0.080 g (65%); m.p. 164 °C; ^{1}H NMR (CD_3CN): δ = 7.71 (t, ^3J = 7.8 Hz, 1H; py), 7.61 (t, ^3J = 6.4 Hz, 2H; NH), 7.25 (d, ^3J = 7.8 Hz, 2H; py), 7.18–7.10 (m, 2H; Ar), 7.03–6.95 (m, 2H; Ar), 6.63–6.55 (m, 4H; Ar), 4.44 (d, ^3J = 6.4 Hz, 4H; CH_2), 3.61 (s, 4H; CH_2), 3.48 (m, 8H; CH_2), 3.59–3.50 (m, 4H; CH_2), 3.35–3.30 (m, 4H; CH_2), 2.78–2.65

(m, 4H; CH_2), 2.53–2.39 ppm (m, 4H; CH_2); ^{13}C NMR (CD_3CN): $\delta =$ 50.5, 54.6, 60.2, 70.6, 71.3, 110.7, 116.8, 120.5, 123.6, 129.3, 130.9, 138.2, 150.2, 160.4 ppm; IR (KBr): $\tilde{\nu} = 3246$ (NH), 1594 (NH), 1594 (C=N)$_{py}$ cm^{-1}; FAB-MS: (m/z): 576 $[L^2+H]^+$; elemental analysis calcd (%) for $C_{33}H_{45}N_5O_4$: C 68.8, H 7.9, N 12.1; found: C 69.0, H 7.5, N 11.9.

X-ray crystal structures: Three-dimensional X-ray data were collected at 100 K on a Bruker X8-APEXII Kappa diffractometer by the Ω/φ scan method. Reflections were measured from a hemisphere of data collected with each frame covering 0.3° in ω. The solution, refinement and analysis of the single-crystal X-ray diffraction data was performed with the WinGX suite for small-molecule single-crystal crystallography.[43] The structure of **1** was solved by Patterson methods with DIRDIF 99[44] and the structure of **2** was solved by direct methods with SHELXS-86,[45] and both were refined by full-matrix least-squares methods on F^2 with SHELXL-97.[46] The hydrogen atoms were included in calculated positions and refined with a riding mode, except hydrogen atoms bonded to the nitrogen atoms, which were found in a Fourier difference map and refined freely. In both crystals some atoms of the aza-crown chain and solvent molecules were disordered. Owing to convergence problems associated with the presence of disordered solvent molecules in special positions, it was necessary to clean up these areas with the program SQUEEZE[47] implemented in PLATON.[48] Finally, the remaining disorder was solved and refinement converged with allowance for thermal anisotropy for all non-hydrogen atoms after imposing 78 restraints for **1** and 3 restraints for **2**. The occupancy factors for the remaining disordered atoms were 0.62(1) for O(1A), O(2A), C(3A) and C(4A) in **1**; and 0.783(4) for atom Br(3A), 0.690 (8) for O(1A), O(2A), C(1A), C(2A), C(3A), C(4A), C(5A) and C(6A) of the crown chain and 0.69(1) for the atoms C(32A) and O(4A) of the methanol molecule in **2**. Crystal data and details on data collection and refinement are summarised in Table 5.

CCDC-671438 and 671439 contain the supplementary crystallographic data for this paper. These data can be obtained free of charge from The Cambridge Crystallographic Data Centre via www.ccdc.cam.ac.uk/data_request/cif.

Computational methods: The $[(H_3L^1)X]^{2+}$ (X = F, Cl, Br or I) and $[(H_3L^1)A]^{2+}$ (A = NO_3 or HSO_4) systems were fully optimised with the B3LYP density functional model.[49,50] We used the standard LanL2DZ basis set in these calculations. The LanL2DZ basis set of Hay and Wadt consists of the D95 basis set for elements of the first row and effective core potentials (ECP) for the core electrons of the Na–Bi elements.[51,52]

Table 5. Crystal data and refinement details for **1** and **2**.

	1	**2**
formula	$C_{31}H_{44}Cl_3N_5O_7$	$C_{32}H_{48}Br_3N_5O_4$
M_r [g mol^{-1}]	705.06	806.48
crystal system	tetragonal	tetragonal
space group	$I4_1/a$	$I4_1/a$
T [K]	100.0 (2)	100.0 (2)
a [Å]	28.8902 (2)	29.0108 (3)
b [Å]	28.8902 (2)	29.0108 (3)
c [Å]	17.4683 (2)	17.1377 (3)
V [Å^3]	14579.8 (2)	14423.5 (3)
$F(000)$	5952	6592
Z	16	16
λ [Å] ($Mo_{K\alpha}$)	0.71073	0.71073
ρ_{calcd} [g cm^{-3}]	1.285	1.486
μ [mm^{-1}]	0.301	3.397
θ range [°]	1.36–28.32	1.38–26.39
R_{int}	0.0557	0.0474
measured reflns	9073	7405
unique reflns	9073	7405
observed reflns [$I > 2\sigma(I)$]	7045	5439
GOF on F^2	1.047	1.082
R_1 [$I > 2\sigma(I)$][a]	0.0511	0.0539
wR_2 (all data)[b]	0.1391	0.1471
largest peak and hole differences [e Å^{-3}]	0.717, −0.593	1.949, −0.713

[a] $R_1 = \Sigma ||F_0| - |Fc|| / \Sigma |F_0|$. [b] $wR_2 = \{\Sigma[w(|F_0|^2 - |Fc|^2)^2] / \Sigma[w(F_o^4)]\}^{1/2}$.

In the case of the $[(H_3L^1)(HSO_4)]^{2+}$ system, the S atom was described with the LanL2DZdp basis set.[53] X-ray structures were used as input geometries when available. The stationary points found on the potential-energy surfaces as a result of the geometry optimisations have been tested to represent energy minima rather than saddle points via frequency analysis. All DFT calculations were performed with the Gaussian 03 program package.[54]

Acknowledgements

The authors thank Xunta de Galicia (PGIDIT06TAM10301PR and Programa Isidro Parga Pondal) and Universidade da Coruña for generous financial support. The authors are indebted to Centro de Supercomputación of Galicia (CESGA) for providing the computer facilities.

[1] a) See special issues on anion coordination chemistry: *Coord. Chem. Rev.* **2003**, *240*, 1–226; *Coord. Chem. Rev.* **2006**, *250*, 2917–3244; b) *Supramolecular Chemistry of Anions* (Eds.: A. Bianchi, K. Bowman-James, E. García-España), Wiley-VCH, New York, **1997**.

[2] R. L. P. Adams, J. T. Knowler, D. P. Leader, *The Biochemistry of Nucleic Acids*, **1986**, Chapman and Hall, New York.

[3] M. Wehner, T. Schrader, *Angew. Chem.* **2002**, *114*, 1827–1831; *Angew. Chem. Int. Ed.* **2002**, *41*, 1751–1754.

[4] J. M. Lehn, *Supramolecular Chemistry: Concepts and Perspectives*, VCH, Weinheim, Germany, **1995**, 59–60.

[5] E. A. Katayev, G. D. Pantos, M. D. Reshetova, V. N. Khrustalev, V. M. Lynch, Y. A. Ustynyuk, J. L. Sessler, *Angew. Chem.* **2005**, *117*, 7552–7556; *Angew. Chem. Int. Ed.* **2005**, *44*, 7386–7390.

[6] G. M Hübner, J. Gläser, C. Seel, F. Vögtle, *Angew. Chem.* **1999**, *111*, 395–398; *Angew. Chem. Int. Ed.* **1999**, *38*, 383–386.

[7] a) L. R. Snyder, J. L. Glajch, J. J. Kirkland, *Practical HPLC Method Development*, Wiley, New York, **1988**; b) P. D. Beer, *Acc. Chem. Res.* **1998**, *31*, 71.

[8] a) S. G. Galbraith, L. F. Lindoy, P. A. Tasker, P. G. Plieger, *Dalton Trans.* **2006**, 1134–1136; b) M. P. Mertes, K. B. Mertes, *Acc. Chem. Res.* **1990**, *23*, 413–418.

[9] a) A. Szumna, J. Jurczak, *Eur. J. Org. Chem.* **2001**, 4031–4039; b) M. J. Chmielewski, J. Jurczak, *Tetrahedron Lett.* **2005**, *46*, 3085–3088; c) M. J. Chmielewski, J. Jurczak, *Chem. Eur. J.* **2005**, *11*, 6080–6094; d) I. V. Korendovych, M. Cho, P. .L. Butler, R. J. Staples, E. V. Rybak-Akimova; e) S. O. Kang, J. M. Llinares, D. Powell, D. VanderVelde, K. Bowman-James, *J. Am. Chem. Soc.* **2003**, *125*, 10152–10153.

[10] C. Kihang, A. D. Hamilton, *J. Am. Chem. Soc.* **2001**, *123*, 2456–2457.

[11] a) S. Mason, J. M. Llinares, M. Morton, T. Clifford, K. Bowman-James *J. Am. Chem. Soc.* **2000**, *122*, 1814–1815; b) C. A. Ilioudis, J. W. Steed, *J. Supramol. Chem.* **2001**, *1*, 165–187.

[12] A. Bencini, A. Bianchi, E. García-España, E. C. Scott, L. Morales, B. Wang, T. Deffo, F. Takusagawa, M. P. Mertes, K. Bowman Mertes, P. Paoletti, *Bioorg. Chem.* **1992**, *20*, 8–29.

[13] Md. A. Hossain, J. M. Llinares, N. W. Alcock, D. Powell, K. Bowman-James, *J. Supramol. Chem.* **2002**, *2*, 143–149.

[14] J. M. Llinares, D. Powell, K. Bowman-James, *Coord. Chem. Rev.* **2003**, *240*, 57–75.

[15] S. O. Kang, Md. A. Hossain, K. Bowman-James, *Coord. Chem. Rev.* **2006**, *250*, 3038–3052.

[16] T. Clifford, A. Danby, J. M. Llinares, S. Mason, N. W. Alcock, D. Powell, J. A. Aguilar, E. García-España, K. Bowman-James, *Inorg. Chem.* **2001**, *40*, 4710–4720.

[17] K. Bowman-James, *Acc. Chem. Res.* **2005**, *38*, 671–678.

[18] C. A. Ilioudis, D. A. Tocher, J. W. Steed, *J. Am. Chem. Soc.* **2004**, *126*, 12395–12402.

[19] B. P. Hay, M. Gutowski, D. A. Dixon, J. Garza, R. Vargas, B. A. Moyer, *J. Am. Chem. Soc.* **2004**, *126*, 7925–7934.

[20] B. P. Hay, D. A. Dixon, J. C. Bryan, B. A. Moyer, *J. Am. Chem. Soc.* **2002**, *124*, 182–183.
[21] J.-M. Lehn, *Pure Appl. Chem.* **1980**, *52*, 2441–2459.
[22] A. Carroy, J.-M. Lehn, *J. Chem. Soc. Chem. Commun.* **1986**, 1232–1234.
[23] S. S. Flack, J.-L. Chaumette, J. D. Kilburn, G. J. Langley, M. Webster, *J. Chem. Soc. Chem. Commun.* **1993**, 399–401.
[24] a) J. M. Mahoney, A. M. Beatty, B. D. Smith, *J. Am. Chem. Soc.* **2001**, *123*, 5847–5848; b) J. M. Mahoney, K. A. Stucker, H. Jiang, I. Carmichael, N. R. Brickmann, A. M. Beatty, B. C. Noll, B. D. Smith, *J. Am. Chem. Soc.* **2005**, *127*, 2922–2928; c) J. M. Mahoney, A. M. Beatty, B. D. Smith, *Inorg. Chem.* **2004**, *43*, 7617–7621; d) J. M. Mahoney, G. U. Nawaratna, A. M. Beatty, P. J. Duggan, B. D. Smith, *Inorg. Chem.* **2004**, *43*, 5902–5907.
[25] a) B. D. Smith, T. N. Lambert, *Chem. Commun.* **2003**, 2261–2268; b) M. J. Deetz, M. Shang, B. D. Smith, *J. Am. Chem. Soc.* **2000**, *122*, 6201–6207; c) J. M. Mahoney, R. A. Marshall, A. M. Beatty, B. D. Smith, S. Camiolo, P. A. Gale, *J. Supramol. Chem.* **2003**, *1*, 289–292; d) A. V. Koulov, J. M. Mahoney, B. D. Smith, *Org. Biomol. Chem.* **2003**, *1*, 27–29.
[26] J. M. Mahoney, J. P. Davis, A. M. Beatty, B. D. Smith, *J. Org. Chem.* **2003**, *68*, 9819–9820.
[27] S.-I. Kondo, Y. Hiraoka, N. Kurumatani, Y. Yano, *Chem. Commun.* **2005**, 1720–1722.
[28] D. A. Nation, J. Reibenspies, A. E. Martell, *Inorg. Chem.* **1996**, *35*, 4597–4603.
[29] K. Nakamoto, *Infrared and Raman Spectra of Inorganic and Coordination Compounds*, 3rd ed., Wiley, New York, **1972**, pp. 142–154.
[30] R. M. Silverstein, C. Bassler, *Spectrometric Identification of Organic Compounds*, Wiley, New York, **1967**.
[31] a) D. Esteban-Gómez, C. Platas-Iglesias, F. Avecilla, A. de Blas, T. Rodríguez-Blas, *Eur. J. Inorg. Chem.* **2007**, 1635–1643; b) F. Avecilla, D. Esteban, C. Platas-Iglesias, S. Fernández-Martínez, A. de Blas, T. Rodríguez-Blas, *Acta Cryst.* **2005**, *C61*, o92-o94.
[32] *Cation Binding by Macrocycles* (Eds.: Y. Inoue, G. W. Gokel), Marcel Dekker, New York, **1990**.
[33] M. A. Hossain, S. O. Kang, D. Powell, K. Bowman-James, *Inorg. Chem.* **2003**, *42*, 1397–1399.
[34] a) E. A. Katayev, N. V. Boev, V. N. Khrustalev, Y. A. Ustynyuk, I. G. Tananaev, J. L. Sessler, *J. Org. Chem.* **2007**, *72*, 2886–2896; b) F. Pichierri, *THEOCHEM* **2002**, *581*, 117–127.
[35] G. R. Desiraju, T. Steiner, *The Weak Hydrogen Bond*, Oxford University Press, **1999**, Chapter 3.
[36] T. Steiner, *Angew. Chem.* **2002**, *114*, 50–80; *Angew. Chem. Int. Ed.* **2002**, *41*, 48–76.
[37] C. Bazzicalupi, A. Bencini, A. Bianchi, A. Danesi, C. Giorgi, M. A. Martínez-Lorente, B. Valtancoli, *New J. Chem.* **2006**, *30*, 959–965.
[38] C. A. Ilioudis, K. S. B. Hancock, D. G. Georganopoulou, J. W. Steed, *New J. Chem.* **2000**, *24*, 787–798.
[39] a) D. Esteban, D. Bañobre, R. Bastida, A. de Blas, A. Macías, A. Rodríguez, T. Rodríguez-Blas, D. E. Fenton, H. Adams, J. Mahía, *Inorg. Chem.* **1999**, *38*, 1937–1944; b) D. Esteban, F. Avecilla, C. Platas-Iglesias, J. Mahía, A. de Blas, T. Rodríguez-Blas, *Inorg. Chem.* **2002**, *41*, 4337–4347.
[40] a) D. Esteban-Gómez, R. Ferreirós, S. Fernández-Martínez, F. Avecilla, C. Platas-Iglesias, A. de Blas, T. Rodríguez-Blas, *Inorg. Chem.* **2005**, *44*, 5428–5436; b) D. Esteban, D. Bañobre, A. de Blas, T. Rodríguez-Blas, R. Bastida, A. Macías, A. Rodríguez, D. E. Fenton, H. Adams, J. Mahía, *Eur. J. Inorg. Chem.* **2000**, 1445–1456.
[41] W. C. Wolsey, *J. Chem. Educ.* **1973**, *50*, A335 A337.
[42] P. Gans, A. Sabatini, A. Vacca, *Talanta* **1996**, *43*, 1739–1753.
[43] WinGX 1.70.01 An integrated system of Windows programs for the solution, refinement and analysis of single-crystal X-ray diffraction data, L. J. Farrugia, *J. Appl. Crystallogr.* **1999**, *32*, 837–838.
[44] P. T.Beurskens, G. Beurskens, R. de Gelder, S. Garcia-Granda, R. O. Gould, R. Israel, J. M. M. Smits, DIRDIF 99 program system, University of Nijmegen, Nijmegen (The Netherlands), **1999**.
[45] G. M. Sheldrick, SHELXS-86, Program for Crystal Structure solution, University of Göttingen, Göttingen (Germany), **1986**.
[46] G. M. Sheldrick,SHELX-97, Programs for Crystal Structure Analysis (Release 97–2), University of Göttingen, Göttingen (Germany), **1998**.
[47] P. v. d. Sluis, A. L. Spek, *Acta Crystallogr. Sect. A* **1990**, *46*, 194–201.
[48] a) A. L.Spek, PLATON, A Multipurpose Crystallographic Tool, Utrecht University, Utrecht (The Netherlands), **2007**; b) A. L. Spek, *J. Appl. Crystallogr.* **2003**, *36*, 7–13.
[49] A. D. Becke, *J. Chem. Phys.* **1993**, *98*, 5648–5652.
[50] C. Lee, W. Yang, R. G. Parr, *Phys. Rev. B* **1988**, *37*, 785–789.
[51] P. J. Hay, W. R. Wadt, *J. Chem. Phys.* **1985**, *82*, 270–283.
[52] A description of the basis sets and theory level used in this work can be found in J. B. Foresman, A. E. Frisch, *Exploring Chemistry with Electronic Structure Methods*, 2nd ed., Gaussian Inc., Pittsburgh, PA, **1996**.
[53] C. E. Check, T. O. Faust, J. M. Bailey, B. J. Wright, T. M. Gilbert, L. S. Sunderlin, *J. Phys. Chem. A* **2001**, *105*, 8111–8116.
[54] Gaussian 03, Revision C.01, M. J. Frisch, G. W. Trucks, H. B. Schlegel, G. E. Scuseria, M. A. Robb, J. R. Cheeseman, J. A. Montgomery, Jr., T. Vreven, K. N. Kudin, J. C. Burant, J. M. Millam, S. S. Iyengar, J. Tomasi, V. Barone, B. Mennucci, M. Cossi, G. Scalmani, N. Rega, G. A. Petersson, H. Nakatsuji, M. Hada, M. Ehara, K. Toyota, R. Fukuda, J. Hasegawa, M. Ishida, T. Nakajima, Y. Honda, O. Kitao, H. Nakai, M. Klene, X. Li, J. E. Knox, H. P. Hratchian, J. B. Cross, V. Bakken, C. Adamo, J. Jaramillo, R. Gomperts, R. E. Stratmann, O. Yazyev, A. J. Austin, R. Cammi, C. Pomelli, J. W. Ochterski, P. Y. Ayala, K. Morokuma, G. A. Voth, P. Salvador, J. J. Dannenberg, V. G. Zakrzewski, S. Dapprich, A. D. Daniels, M. C. Strain, O. Farkas, D. K. Malick, A. D. Rabuck, K. Raghavachari, J. B. Foresman, J. V. Ortiz, Q. Cui, A. G. Baboul, S. Clifford, J. Cioslowski, B. B. Stefanov, G. Liu, A. Liashenko, P. Piskorz, I. Komaromi, R. L. Martin, D. J. Fox, T. Keith, M. A. Al-Laham, C. Y. Peng, A. Nanayakkara, M. Challacombe, P. M. W. Gill, B. Johnson, W. Chen, M. W. Wong, C. Gonzalez, J. A. Pople, Gaussian, Inc., Wallingford CT, **2004**.

Received: January 16, 2008
Published online: May 21, 2008

